The Astronomical Journal, 156:299 (8pp), 2018 December https://doi.org/10.3847/1538-3881/aaee6d

Kinematics of Type II Cepheids of the Galactic Halo

George Wallerstein and Elizabeth M. Farrell
Department of Astronomy, University of Washington, Seattle, WA 98195, USA
Received 2018 October 9; revised 2018 November 1; accepted 2018 November 2; published 2018 December 6

Abstract

In a step toward understanding the origin of the Galactic Halo, we have reexamined Type II Cepheids (T2C) in the field with new input from the second data release (DR2) of *Gaia*. For 45 T2C with periods from 1 to 20 days, parallaxes, proper motions, and [Fe/H] values are available for 25 stars. Only five show [Fe/H] < -1.5, while the remaining stars show thick disk kinematics and [Fe/H] > -0.90. We have compared the T2C stars of the field with their cousins in the globular clusters of the Halo and found that the globular clusters with T2C stars show metallicities and kinematics of a pure Halo population. The globular cluster may have formed during the overall collapse of the Galaxy, while the individual thick disk T2C stars may have been captured from small systems that self-enriched prior to capture. The relationship of these two populations to the microgalaxies currently recognized as surrounding the Galaxy is unclear.

Key words: Galaxy: halo – globular clusters: general – stars: variables: Cepheids

1. Introduction

The concept of stellar populations was introduced by Baade (1944), who called attention to the differences between stars in the spiral arms of galaxies as compared to galactic halos and bulges. At the Vatican Conference (O'Connell 1958), the concepts of halo, thick disk, thin disk, and spiral arms were specified. The Halo was defined by the globular clusters and stars whose motions carried them to large distances above the Galactic Plane. Metallicity studies by Chamberlain & Aller (1951), Schwarzschild et al. (1957), and Helfer et al. (1959) showed that both individual stars and globular clusters of the halo are deficient in metals by factors as large as 100. Subsequent surveys of individual stars and integrated light of globular cluster showed a substantial range in metallicity (Deutsch 1955, Kinman 1959). The assignment of a star, or a group of stars, to a specific population involves both the location and kinematics of the star or group. It is preferable to employ metallicity as a property of a population rather than as a defining parameter.

Once the difference between Classical Cepheids and Cepheids in globular clusters had been recognized by Baade (1956), the T2C stars seemed to be tracers of the Halo. At that time, the T2C stars were mostly too faint for high-dispersion analysis of their metallicity, but their radial velocities could be measured. Using their velocities and positions, Woolley (1966) concluded that most, but not all, of the T2C stars at substantial galactic latitudes belonged to the thick disk population rather than to the Halo population and its globular cluster T2C stars. T2C stars are also found in the Large and Small Magellanic Clouds (Soszyński et al. 2008, 2010), but their velocities and metallicities have not been evaluated because of their faintness. In this paper, we present kinematic and metallicity data for individual T2C stars in the field, and compare their properties with T2C stars in globular clusters.

2. Observations

The second data release of *Gaia* provides a substantial upgrade in the available data for T2C stars in the Galactic Halo. Over the 50 years since Woolley's paper, many Cepheids have been found at substantial distances above the Galactic Plane. In the General Catalog of Variable Stars (Samus et al. 2001), they are listed as CW stars. The Catalog of H. C. Harris (1985), and new identifications by Schmidt et al. (2003a, 2003b, 2004), have provided a substantial database for T2C stars in the field. Metallicities have been provided by Maas et al. (2007), Schmidt et al. (2003b), Harris (1981), Kovtyukh et al. (2018b), and Lemasle et al. (2015). So as to avoid the Galactic Bulge, we have excluded from our list stars with a galactic longitude between 350° and 10°, and with a galactic latitude less than ±10°. Only the stars whose parallax exceeds the probable error of their parallax by a factor of at least five have been included.[1]

The distances and proper motions of T2C stars had been largely unknown until *Gaia* DR2 (Luri et al. 2018). Hence, we have assembled a list of T2C field stars with their periods, distances, absolute magnitudes, and metallicities. Our assembled data for T2C stars in the galactic field are shown in Table 1. We plotted [Fe/H] against period for each T2C star in the field in Figure 1, where we separate the halo and disk Cepheids by [Fe/H] $= -1.0$.

For the globular clusters, data are to be found in the catalog of C. Clement (updated 2017 January), combined with the catalogs of H. Sawyer Hogg (Clement et al. 2001), which includes the metallicities of each cluster with a T2C star. We have omitted the cluster Omega Cen, and the 2 unusual globular cluster NGC 6388 and NGC 6441, as they are probably the remains of elliptical galaxies (Corwin et al. 2006).[2] For the T2C stars in the Galactic Bulge, see the paper by Bhardwaj et al. (2017). A few stars with periods over 20

[1] There is no simple way to balance the need to include as much data as possible without including data with an undesirable level of uncertainty. For a discussion of parallax errors, see Luri et al. (2018), Bailer-Jones et al. (2018), as well as Lutz & Kelker (1973).

[2] Omega Cen is a special environment for variable stars because it seems to contain stars with [Fe/H] from 0.0 to −2.5. According to Clement et al. (2001), it has nine stars classified as Cepheids, and one RV Tau star. According to Gonzalez & Wallerstein (1994), variables 1, 29, and 48 have [Fe/H] values of −1.77, −1.99, and −1.65, respectively. Two other stars that lie to the left of the red gaint branch, ROA 24 and 342 have [Fe/H] = −2.05 and −1.97. Thus, Omega Cen, despite its very wide range in metallicity, shows only metal-poor variables, and similar stars that lie above, or to the left of, the red giant branch.

Table 1
Field Type II Cepheids from *Gaia*

Star	P(days)	π(mas)	M_G	[Fe/H]
BX Del	1.092	0.343 ± 0.039	−0.132	−0.20
V716 Oph	1.116	0.359 ± 0.045	−0.159	−1.64
BF Ser	1.165	0.247 ± 0.036	−0.925	−2.08
VY Pyx	1.200	3.902 ± 0.053	0.036	−0.40
CE Her	1.209	0.200 ± 0.036	−0.973	−1.80
BV Cha	1.238	0.365 ± 0.026	−0.005	⋯
BL Her	1.307	0.793 ± 0.031	−0.312	−0.10
XX Vir	1.348	0.312 ± 0.040	−0.139	−1.57
MQ Aql	1.481	0.095 ± 0.025	−1.294	⋯
KZ Cen	1.520	0.248 ± 0.036	−0.607	⋯
SW Tau	1.584	1.115 ± 0.051	−0.194	0.20
V745 Oph	1.595	0.190 ± 0.027	−0.473	−0.70
NW Lyr	1.601	0.319 ± 0.029	−0.139	−0.10
V971 Aql	1.625	0.567 ± 0.053	0.579	−0.30
DU Ara	1.641	0.418 ± 0.040	0.044	⋯
VZ Aql	1.668	0.232 ± 0.027	0.170	0.30
V439 Oph	1.893	0.488 ± 0.034	0.291	−0.30
RT TrA	1.946	1.027 ± 0.091	−0.322	⋯
V553 Cen	2.060	1.718 ± 0.076	−0.551	0.01
UY Eri[a]	2.213	0.248 ± 0.057	−1.771	−1.80
AU Peg	2.402	1.674 ± 0.045	0.171	0.27
CN CMa	2.546	0.196 ± 0.025	−0.295	⋯
V351 Cep	2.806	0.496 ± 0.039	−2.383	⋯
BE Pup	2.871	0.156 ± 0.024	−0.764	⋯
LN Pav	3.600	0.896 ± 0.022	3.309	⋯
BD Cas	3.652	0.327 ± 0.028	−1.960	⋯
V383 Cyg	4.612	0.475 ± 0.027	−1.497	⋯
V394 Cep	5.689	0.105 ± 0.021	−1.729	⋯
TX Del	6.166	0.978 ± 0.040	−0.988	0.10
PZ Aql	8.756	0.525 ± 0.040	−0.426	⋯
V1043 Cyg	8.847	0.214 ± 0.029	−1.230	⋯
κ Pav	9.094	5.199 ± 0.309	0.336	0.10
IX Cas	9.155	0.222 ± 0.037	−2.007	−0.40
AL Vir	10.303	0.346 ± 0.047	−2.918	−0.38
AP Her	10.416	0.343 ± 0.038	−1.709	−0.70
CQ Cha	12.300	0.497 ± 0.018	1.468	⋯
AL Lyr	12.992	0.228 ± 0.027	−1.529	⋯
DD Vel	13.195	0.454 ± 0.031	0.032	−0.48
V2338 Oph	13.700	0.260 ± 0.035	−1.334	⋯
FI Sct	14.862	0.168 ± 0.032	−0.410	⋯
CO Pup	16.019	0.263 ± 0.027	−2.123	−0.60
W Vir	17.274	0.399 ± 0.066	−1.927	−0.67
ST Pup	19.000	0.371 ± 0.026	−2.113	−0.90
CY Vel	19.529	0.174 ± 0.027	−1.338	⋯
RS Pav	19.954	0.353 ± 0.037	−1.870	⋯

Note.
[a] Despite the fact that UY Eri has a probable error only 4.35 times its parallax, it has been included, as it is used to define a class of stars.

days have been excluded because they are rare and may show RV Tau behavior.[3]

To compare the field and globular cluster T2C stars, we plotted [Fe/H] against period for each star that is a cluster member in Figure 2.

Globular clusters show an absence of T2C stars with periods between about 3 and 9 days, with the exception of variable 3 in M10, and variable 2 in M13, which fall in the middle of the gap for variables in globular clusters. The field stars show a deficiency of variables with [Fe/H] < -1.0, with the exception of a small clump with periods between 1 and 3 days, and [Fe/H] between −1.5 and −2.0 recently analyzed by Kovtyukh et al. (2018a) and called UY Eridani stars. Short period T2C stars with significantly larger metallicities are usually called BL Herculis stars.

3. Kinematics of T2C Stars in the Field

Stellar populations are closely associated with the galactic orbits of the objects in question. Their stellar motions with respect to the local standard of rest (LSR) may best be parameterized by their U, V, W components of motion, where the component U is positive toward the Galactic Anticenter, V is positive in the direction of Galactic Rotation, and W is positive toward the North Galactic Pole. In Table 2, we show the U, V, W, components for each T2C star with a parallax of at least five times its probable error in the *Gaia* catalog. The U, V, W components of motion were calculated using the gal_uvw script (Koposov 2016)[4] available on GitHub, which follows the outline of Johnson & Soderblom (1987), except that U is positive toward the Galactic Anticenter, rather than the Galactic Center, and the J2000 transformation matrix to galactic coordinates was taken from the *Hipparcos* and Tycho Catalogs (ESA 1997). Radial velocities were taken from *Gaia* DR2, Beers et al. (2000), Kordopatis et al. (2013), Kharchenko et al. (2007), and Barbier-Brossat et al. (1994). The radial velocities in *Gaia* DR2 are preliminary, because they were measured during each visit with the *Gaia* spectrograph, which covers a wavelength from 8500 to 8900 Å with a resolution of 11000, just as the Radial Velocity Experiment did. In Figure 3, we show the dependence of the U, V, and W components on the metallicity of each star. The distribution of the W components is the most important for distinguishing the population of halo stars. T2C stars with [Fe/H] from 0.0 to −1.0, show a distribution from −60 to 100 km s^{-1}, with single outliers near −100 and 180 km s^{-1}. For the metal-poor stars with [Fe/H] < -1.5, the W components lie from −100 to 100. It is interesting to note the large negative V components for the metal-poor stars, indicating that their orbits are retrograde and the stars must have been captured. Despite the current century being called the "era of big data", there are so few stars in this category that little is proven from this sample.

4. Kinematics of T2C in Globular Clusters

We can still compare the small sample of T2C stars with globular clusters that contain Cepheids as shown on the right side of Figure 3, where the data for their distances, proper motions, and radial velocities have been obtained from the Gaia Collaboration (2018) and Harris (1996).

In Table 3, we show the kinematics of globular clusters with at least 1 T2C star. The sample of T2C stars in globular clusters must be nearly complete due to the many investigations of variable stars in clusters. They are found in globular cluster with [Fe/H] $\leqslant -1.0$.

There are other environments with T2C stars including the Large Magellanic Cloud (Soszyński et al. 2008), the Small Magellanic Cloud (Soszyński et al. 2010), the Fornax system (Bersier & Wood 2002), and the Galactic Bulge (Bhardwaj et al. 2017), but none of them have been investigated for their metallicity.

[3] RV Tau behavior is defined as alternating low and high minimum light. It is usually seen in T2C stars with periods greater than 20 days; however, the term has also been used for T2C stars with periods greater than 20 days, even though their minima have not shown alteration.

[4] github.com/segasai/astrolibpy/blob/master/astrolib/gal_uvw.py

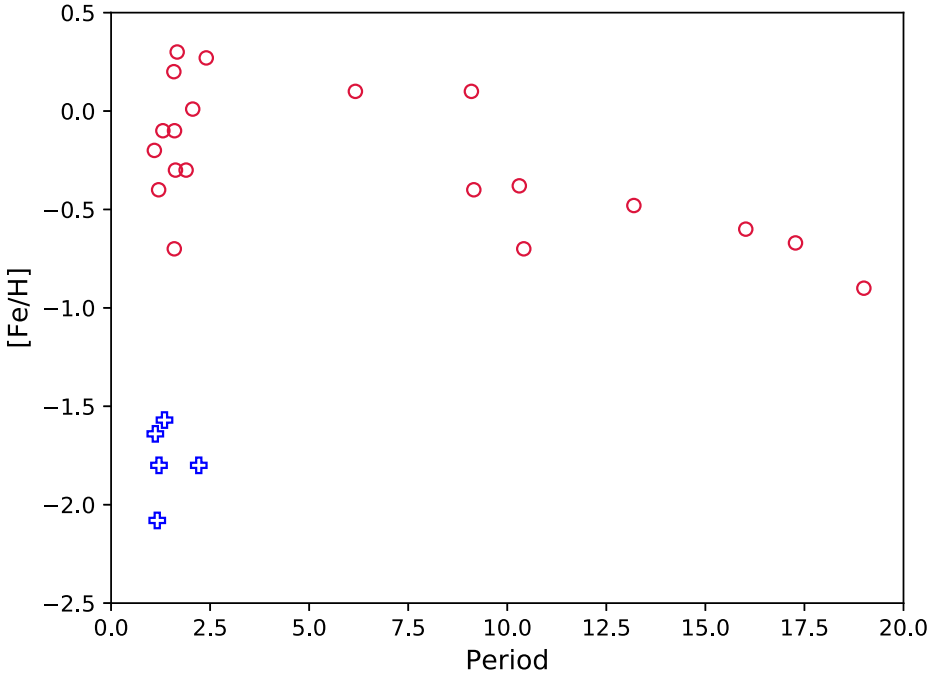

Figure 1. Type II Cephieds in the Galactic disk and Halo. Disk Cephieds are represented by red markers, while halo Cepheids are represented by blue markers. They are separated by [Fe/H] = −1.0.

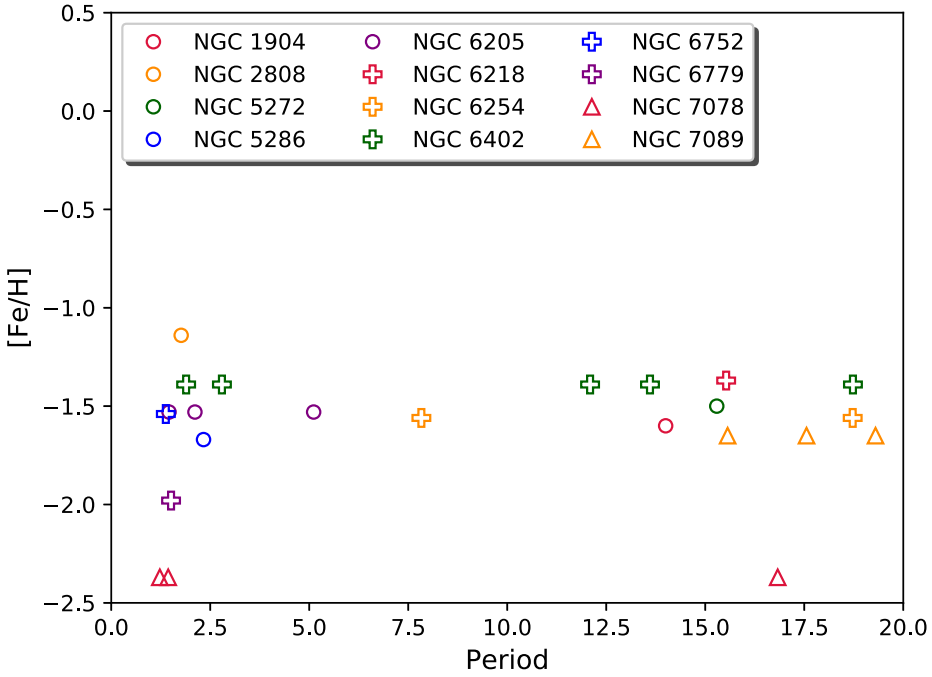

Figure 2. Globular cluster with type II Cepheids.

In Table 4, we show the kinematics of globular clusters that lack T2C stars.

5. Discussion

An examination of Figure 3 permits the following relationships between T2C stars in the field and in globular clusters:

1. There are no globular clusters with [Fe/H] > −1.0 and a T2C star (excluding Omega Cen, NGC 6388, and NGC 6441).
2. The field T2C stars are rather well clumped in the *U*, *V*, and particularly *W* components.
3. Globular clusters with T2C stars have widely spread *U*, *V*, and *W* velocities.
4. Non-bulge globular cluster without Cepheids show a wide range in *U* and *V* components, and a significant range in *W*, which means a wide range in height above of below the Galactic Plane to which they penetrate. It was on this basis that the globular cluster have been used to define Population II.

Table 2
Kinematics of Field Type II Cepheids

Star	l(deg)	b(deg)	$\mu_{\alpha*}$(mas yr^{-1})	μ_δ(mas yr^{-1})	v_r(km s^{-1})	U(km s^{-1})	V(km s^{-1})	W(km s^{-1})
BX Del	59.939	−10.281	−1.142 ± 0.054	−6.530 ± 0.054	−6.964 ± 7.344	$-74.604^{+07.920}_{-09.952}$	$-40.292^{+05.309}_{-06.672}$	$-28.035^{+03.463}_{-04.351}$
V716 Oph	9.857	27.795	−25.789 ± 0.072	−7.152 ± 0.039	−230.000 ± 30.000	$249.531^{+06.466}_{-08.319}$	$-306.850^{+32.668}_{-42.032}$	$99.525^{+22.694}_{-29.199}$
BF Ser	22.865	54.822	−15.362 ± 0.055	−13.289 ± 0.069	−146.084 ± 9.678	$56.735^{+01.842}_{-02.471}$	$-397.089^{+49.491}_{-66.379}$	$-17.449^{+12.358}_{-16.575}$
VY Pyx	248.771	13.617	10.996 ± 0.067	29.424 ± 0.052	21.031 ± 1.931	$14.659^{+00.220}_{-00.226}$	$8.675^{+00.170}_{-00.175}$	$43.098^{+00.325}_{-00.334}$
CE Her	39.125	22.037	−2.289 ± 0.055	−3.359 ± 0.068	−258.000 ± 30.000	$122.473^{+09.255}_{-13.318}$	$-215.201^{+13.273}_{-19.100}$	$-73.779^{+02.953}_{-04.250}$
BV Cha	303.439	−16.896	−2.348 ± 0.053	−1.322 ± 0.042	−0.628 ± 4.089	$20.419^{+02.532}_{-02.921}$	$0.507^{+01.139}_{-01.314}$	$-8.448^{+01.465}_{-01.690}$
BL Her	45.161	19.463	−4.140 ± 0.042	−11.750 ± 0.060	19.031 ± 5.429	$-74.923^{+02.481}_{-02.294}$	$-25.247^{+02.426}_{-02.243}$	$8.577^{+00.083}_{-00.077}$
XX Vir	337.777	50.717	−11.460 ± 0.080	−10.899 ± 0.070	−55.000 ± 30.000	$74.236^{+07.876}_{-06.086}$	$-205.947^{+35.976}_{-27.799}$	$-69.773^{+05.167}_{-03.993}$
MQ Aql	49.842	−4.960	−10.423 ± 0.038	−7.598 ± 0.034	…	…	…	…
KZ Cen	294.076	15.740	8.054 ± 0.049	−3.898 ± 0.034	201.967 ± 3.588	$-243.761^{+25.747}_{-19.220}$	$-107.048^{+09.073}_{-06.773}$	$20.362^{+07.875}_{-05.878}$
SW Tau	190.140	−29.867	3.892 ± 0.109	−8.803 ± 0.062	10.900 ± 0.300	$-10.031^{+00.784}_{-00.715}$	$-27.180^{+01.767}_{-01.613}$	$-5.588^{+00.801}_{-00.731}$
V745 Oph	25.654	22.033	−0.178 ± 0.046	−10.354 ± 0.041	…	…	…	…
NW Lyr	66.477	10.350	2.042 ± 0.044	−3.372 ± 0.048	−10.771 ± 7.991	$-36.973^{+04.184}_{-03.486}$	$-0.933^{+00.917}_{-00.764}$	$-43.831^{+04.539}_{-03.783}$
V971 Aql	26.992	−12.585	−5.848 ± 0.091	−0.047 ± 0.074	−40.710 ± 10.377	$8.615^{+02.419}_{-02.006}$	$-19.481^{+02.355}_{-01.953}$	$58.212^{+04.869}_{-04.036}$
DU Ara	327.931	−15.214	−1.923 ± 0.036	−6.997 ± 0.043	−21.591 ± 4.232	$56.190^{+05.323}_{-04.393}$	$-39.489^{+07.369}_{-06.082}$	$-9.590^{+02.199}_{-01.815}$
VZ Aql	28.359	−6.133	−2.428 ± 0.049	−4.457 ± 0.046	105.000 ± NaN	$-149.926^{+07.270}_{-05.754}$	$-28.068^{+13.247}_{-10.485}$	$-1.308^{+00.982}_{-00.777}$
V439 Oph	28.317	16.729	−3.531 ± 0.053	−11.534 ± 0.051	−69.547 ± 8.315	$-9.844^{+04.774}_{-04.152}$	$-116.874^{+08.062}_{-07.012}$	$-33.495^{+01.258}_{-01.094}$
RT TrA	325.258	−10.400	−3.374 ± 0.098	−11.447 ± 0.078	−7.249 ± 6.765	$29.248^{+03.440}_{-02.880}$	$-21.122^{+04.274}_{-03.578}$	$-15.227^{+02.131}_{-01.784}$
V553 Cen	329.579	24.677	4.012 ± 0.164	−1.689 ± 0.175	−6.000 ± 2.700	$-11.771^{+00.081}_{-00.074}$	$20.231^{+00.402}_{-00.368}$	$-4.075^{+00.594}_{-00.544}$
UY Eri	193.341	−52.629	24.426 ± 0.076	−6.348 ± 0.095	177.327 ± 8.515	$274.845^{+50.871}_{-31.857}$	$-410.894^{+119.681}_{-074.947}$	$68.693^{+58.895}_{-36.882}$
AU Peg	69.130	−22.266	−2.730 ± 0.070	−12.887 ± 0.079	0.000 ± 4.400	$-36.584^{+01.063}_{-01.008}$	$-4.636^{+00.606}_{-00.574}$	$-10.191^{+00.457}_{-00.433}$
CN CMa	231.503	−4.500	−0.652 ± 0.036	1.708 ± 0.033	…	…	…	…
V351 Cep	105.151	−0.719	−3.352 ± 0.070	−1.614 ± 0.063	−21.214 ± 4.971	$-48.249^{+03.843}_{-03.283}$	$2.203^{+01.041}_{-00.889}$	$9.552^{+00.039}_{-00.034}$
BE Pup	240.555	−2.997	−1.252 ± 0.034	1.765 ± 0.040	116.229 ± 7.586	$105.258^{+09.680}_{-07.099}$	$-55.241^{+05.652}_{-04.145}$	$-7.059^{+03.118}_{-02.287}$
LN Pav	325.613	−28.320	2.246 ± 0.025	1.086 ± 0.034	…	…	…	…
BD Cas	117.994	−0.958	−1.936 ± 0.044	−0.923 ± 0.040	−49.300 ± 0.300	$-58.064^{+03.177}_{-02.676}$	$-16.263^{+01.663}_{-01.401}$	$-1.383^{+01.328}_{-01.119}$
V383 Cyg	73.927	−2.765	−0.620 ± 0.045	−3.943 ± 0.042	−24.400 ± 0.300	$-35.673^{+02.660}_{-02.374}$	$-20.715^{+00.814}_{-00.727}$	$-10.282^{+00.955}_{-00.852}$
V394 Cep	102.939	3.299	−2.348 ± 0.039	−1.448 ± 0.037	…	…	…	…
TX Del	50.958	−24.263	−2.989 ± 0.067	−7.693 ± 0.046	13.594 ± 2.887	$-44.895^{+01.554}_{-01.432}$	$-4.135^{+01.342}_{-01.237}$	$-5.911^{+00.141}_{-00.130}$
PZ Aql	30.880	−2.312	0.241 ± 0.104	−7.587 ± 0.087	−6.282 ± 5.744	$-32.770^{+03.090}_{-02.652}$	$-42.037^{+05.341}_{-04.585}$	$-26.331^{+02.210}_{-01.897}$
V1043 Cyg	75.125	1.960	−3.601 ± 0.045	−6.295 ± 0.053	−16.388 ± 3.563	$-159.334^{+26.011}_{-19.803}$	$-43.266^{+06.859}_{-05.222}$	$-4.316^{+01.392}_{-01.060}$
κ Pav	328.287	−25.388	−8.957 ± 0.325	15.091 ± 0.376	37.800 ± 0.800	$-47.734^{+00.516}_{-00.458}$	$3.401^{+00.096}_{-00.085}$	$-0.294^{+00.819}_{-00.727}$
IX Cas	115.347	−11.949	−4.481 ± 0.045	−1.980 ± 0.036	−104.000 ± 2.900	$-146.204^{+20.068}_{-14.335}$	$-39.470^{+08.248}_{-05.891}$	$4.555^{+05.373}_{-03.838}$
AL Vir	330.999	45.173	−4.755 ± 0.084	−0.072 ± 0.072	14.393 ± 4.327	$28.179^{+07.698}_{-05.857}$	$-34.011^{+08.314}_{-06.326}$	$35.833^{+02.685}_{-02.043}$
AP Her	47.090	7.404	−2.325 ± 0.062	−6.991 ± 0.069	−31.865 ± 5.557	$-62.086^{+10.339}_{-08.276}$	$-77.152^{+09.378}_{-07.507}$	$-11.281^{+01.314}_{-01.052}$
CQ Cha	302.860	−15.062	−10.049 ± 0.031	4.580 ± 0.032	…	…	…	…
AL Lyr	60.592	6.583	−1.896 ± 0.036	−1.267 ± 0.045	−3.608 ± 4.952	$-41.563^{+05.823}_{-04.590}$	$-12.398^{+03.724}_{-02.936}$	$28.925^{+03.337}_{-02.630}$
DD Vel	271.505	−1.387	−1.026 ± 0.054	−1.857 ± 0.058	36.235 ± 3.346	$-16.196^{+00.552}_{-00.481}$	$-22.144^{+00.073}_{-00.064}$	$-15.477^{+02.432}_{-02.121}$
V2338 Oph	34.847	13.786	−3.866 ± 0.059	−13.087 ± 0.059	−166.727 ± 4.592	$-23.917^{+23.909}_{-18.235}$	$-274.769^{+31.874}_{-24.310}$	$-73.717^{+05.743}_{-04.380}$
FI Sct	26.502	−1.858	−1.225 ± 0.050	−4.975 ± 0.048	…	…	…	…
CO Pup	250.444	4.521	−4.445 ± 0.037	5.822 ± 0.036	77.644 ± 5.122	$141.862^{+14.112}_{-11.484}$	$-15.775^{+04.878}_{-03.970}$	$7.559^{+01.599}_{-01.301}$
W Vir	319.566	58.371	−3.944 ± 0.094	1.027 ± 0.102	−59.017 ± 17.301	$57.818^{+08.866}_{-06.349}$	$14.457^{+05.619}_{-04.024}$	$-31.303^{+01.912}_{-01.369}$
ST Pup	246.852	−16.492	−0.660 ± 0.043	3.613 ± 0.047	45.000 ± 1.000	$51.791^{+02.828}_{-02.458}$	$-10.660^{+01.235}_{-01.073}$	$2.689^{+00.080}_{-00.070}$
CY Vel	273.397	−3.9341	−3.670 ± 0.047	6.256 ± 0.041	61.578 ± 5.557	$180.574^{+35.453}_{-25.928}$	$-62.229^{+02.489}_{-01.820}$	$43.540^{+05.575}_{-04.077}$
RS Pav	335.010	−17.638	−2.054 ± 0.058	−0.761 ± 0.054	10.000 ± NaN	$-14.346^{+00.657}_{-00.533}$	$-11.842^{+03.531}_{-02.861}$	$23.664^{+02.817}_{-02.283}$

Note. Type II Cepheids are ordered by period, as they are in Table 1.

5. As shown by their V components, the five halo T2C stars appear to be in retrograde orbits, indicating that they are captured.

6. Conclusions

We confirm the suggestion by Woolley (1966) that most of the T2C field stars of the Galactic Halo belong to a different population than the globular clusters of the Halo. This raises a number of questions as to the origin of the Halo.

The origin of the Galactic Halo has been an important aspect of research on galactic structure ever since the Vatican Conference (O'Connell 1958). Two different approaches have been suggested: the model of Eggen et al. (1962), which suggests that the Halo consists of material left behind as the galaxy contracted to a central bulge with spiral arms, and that of Searle & Zinn (1978), who proposed a model in which the Halo consists of small systems that have been captured over time by the galaxy's gravitational field. The latter is supported by the discovery of fragments such as those described by

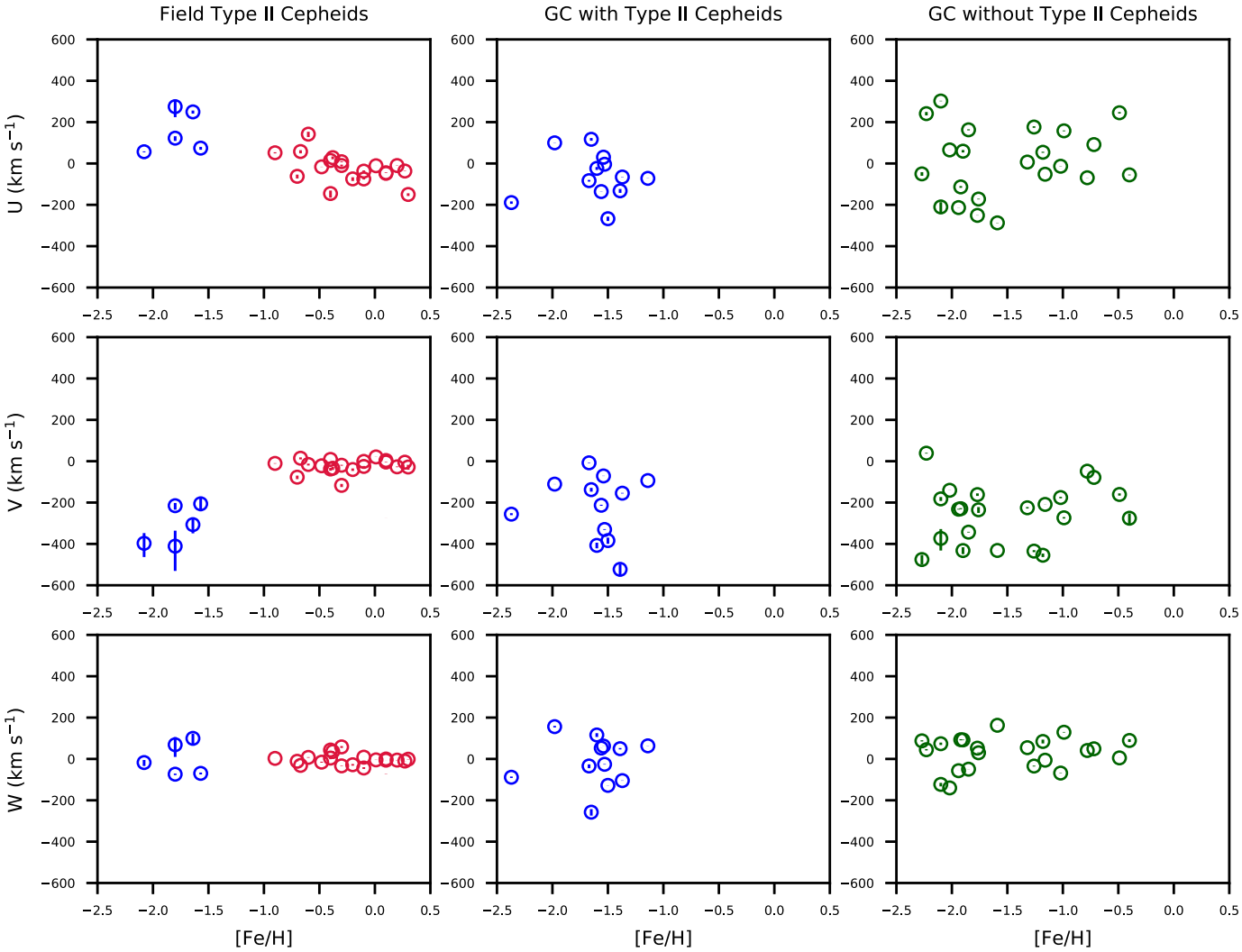

Figure 3. *U, V, W* components of T2C in the galactic field, globular clusters, and globular clusters without Cepheids.

Willman (2010) and many others over the past decade (McConnachie 2012), most recently, Myeong et al. (2018).

Of the various stellar types found in the Halo, the T2C stars have the highest visual luminosity and are easy to recognize by their periods from 1 to 20 days. However, it is surprising that the two elliptical companions to M31, NGC 147 and NGC 185, do not have any T2C stars at all (Monelli et al. 2017) despite the presence of many RR Lyrae stars in both galaxies. In addition, a search for variables in six small companion galaxies of M31 revealed 870 RR Lyrae stars, and 15 anomalous Cepheids, but not a single recognized T2C star (Martínez-Vázquez et al. 2017). A search for T2C stars in the giant ellipticals in nearby galaxy clusters would require photometry down to $V = 28$, and probably a telescope of 30 m aperture. In the meantime, we await the discovery of additional T2C stars in our galaxy with *Gaia*, Pan-STARRS, and the Large Synoptic Survey Telescope (LSST).

This work has made use of data from the European Space Agency (ESA) mission *Gaia* (https://www.cosmos.esa.int/gaia), processed by the *Gaia* Data Processing and Analysis Consortium (DPAC, https://www.cosmos.esa.int/web/gaia/dpac/consortium). Funding for the DPAC has been provided by national institutions, in particular the institutions participating in the *Gaia* Multilateral Agreement.

Table 3
Kinematics of Globular Clusters with Type II Cepheids

Cluster	[Fe/H]	l(deg)	b(deg)	π(mas)	$\mu_{\alpha*}$(mas yr^{-1})	μ_δ(mas yr^{-1})	v_r(km s^{-1})	U(km s^{-1})	V(km s^{-1})	W(km s^{-1})
NGC 1904	−1.60	227.229	−29.352	0.036 ± 0.002	2.470 ± 0.005	−1.560 ± 0.005	206.430 ± 0.870	$-23.722^{+07.420}_{-06.754}$	$-407.100^{+14.236}_{-12.959}$	$115.874^{+09.625}_{-08.761}$
NGC 2808	−1.14	282.193	−11.253	0.056 ± 0.001	1.003 ± 0.003	0.279 ± 0.003	104.610 ± 1.260	$-71.967^{+00.456}_{-00.446}$	$-93.611^{+00.005}_{-00.005}$	$63.373^{+00.458}_{-00.448}$
NGC 5272	−1.50	42.217	78.707	0.027 ± 0.001	−0.113 ± 0.003	−2.627 ± 0.002	−146.480 ± 0.660	$-267.127^{+10.820}_{-10.033}$	$-383.906^{+15.473}_{-14.348}$	$-127.833^{+00.476}_{-00.441}$
NGC 5286	−1.67	311.614	10.568	0.017 ± 0.003	0.184 ± 0.008	−0.148 ± 0.007	56.800 ± 1.660	$-83.016^{+04.544}_{-03.367}$	$-7.833^{+01.406}_{-01.041}$	$-34.063^{+10.542}_{-07.811}$
NGC 6205	−1.53	59.009	40.912	0.080 ± 0.001	−3.176 ± 0.003	−2.588 ± 0.003	−245.620 ± 0.940	$-3.778^{+00.921}_{-00.905}$	$-330.195^{+01.806}_{-01.775}$	$-25.896^{+01.239}_{-01.217}$
NGC 6218	−1.37	15.715	26.313	0.156 ± 0.001	−0.158 ± 0.004	−6.768 ± 0.003	−41.000 ± 0.510	$-65.411^{+00.785}_{-00.772}$	$-154.608^{+01.462}_{-01.438}$	$-104.793^{+00.727}_{-00.715}$
NGC 6254	−1.56	15.137	23.076	0.151 ± 0.001	−4.703 ± 0.004	−6.529 ± 0.003	76.760 ± 0.590	$-135.877^{+00.567}_{-00.557}$	$-213.050^{+02.429}_{-02.385}$	$52.518^{+00.204}_{-00.200}$
NGC 6402	−1.39	21.324	14.804	0.054 ± 0.003	−3.615 ± 0.007	−5.036 ± 0.006	−66.100 ± 1.800	$-132.245^{+09.941}_{-08.988}$	$-523.037^{+27.978}_{-25.294}$	$49.607^{+03.451}_{-03.120}$
NGC 6752	−1.54	336.493	−25.628	0.231 ± 0.001	−3.191 ± 0.002	−4.035 ± 0.002	−26.120 ± 0.510	$30.680^{+00.091}_{-00.091}$	$-71.282^{+00.498}_{-00.494}$	$62.372^{+00.240}_{-00.237}$
NGC 6779	−1.98	62.659	8.336	0.070 ± 0.002	−2.009 ± 0.005	1.65 ± 0.006	−136.670 ± 1.000	$99.811^{+00.571}_{-00.547}$	$-110.823^{+00.338}_{-00.324}$	$156.236^{+03.842}_{-03.682}$
NGC 7078	−2.37	65.013	−27.313	0.057 ± 0.001	−0.624 ± 0.004	−3.796 ± 0.004	−105.580 ± 1.450	$-189.127^{+06.013}_{-05.724}$	$-256.021^{+04.838}_{-04.605}$	$-88.500^{+03.573}_{-03.401}$
NGC 7089	−1.65	53.371	−35.770	0.059 ± 0.004	3.491 ± 0.008	−2.150 ± 0.007	−4.790 ± 0.270	$116.961^{+06.981}_{-06.201}$	$-137.525^{+09.720}_{-08.633}$	$-257.455^{+16.618}_{-14.760}$

Table 4
Kinematics of Globular Clusters without Type II Cepheids

Cluster	[Fe/H]	l(deg)	b(deg)	π(mas)	$\mu_{\alpha*}$(mas yr^{-1})	μ_{δ}(mas yr^{-1})	v_r(km s^{-1})	U(km s^{-1})	V(km s^{-1})	W(km s^{-1})
NGC 0104	−0.72	305.895	−72.082	0.196 ± 0.000	5.248 ± 0.002	−2.519 ± 0.002	−18.950 ± 0.420	$91.394^{+00.050}_{-00.050}$	$-78.301^{+00.109}_{-00.109}$	$49.102^{+00.059}_{-00.059}$
NGC 0288	−1.32	151.285	−89.380	0.140 ± 0.002	4.239 ± 0.004	−5.647 ± 0.003	−49.060 ± 0.320	$6.920^{+00.089}_{-00.092}$	$-225.250^{+03.529}_{-03.637}$	$54.469^{+00.017}_{-00.018}$
NGC 0362	−1.26	301.533	−46.247	0.079 ± 0.001	6.695 ± 0.005	−2.518 ± 0.003	226.930 ± 0.770	$176.241^{+03.695}_{-03.809}$	$-434.817^{+04.683}_{-04.828}$	$-34.436^{+01.972}_{-02.033}$
NGC 1851	−1.18	244.513	−35.036	0.030 ± 0.001	2.131 ± 0.004	−0.622 ± 0.004	323.360 ± 1.040	$54.251^{+02.460}_{-02.648}$	$-454.826^{+08.052}_{-08.669}$	$84.532^{+08.857}_{-09.536}$
NGC 2298	−1.92	245.629	−16.006	0.079 ± 0.002	3.276 ± 0.006	−2.191 ± 0.006	147.410 ± 1.400	$-113.330^{+04.063}_{-04.263}$	$-229.676^{+02.640}_{-02.770}$	$92.866^{+02.537}_{-02.662}$
NGC 3201	−1.59	277.229	8.640	0.172 ± 0.001	8.334 ± 0.002	−1.990 ± 0.002	494.620 ± 0.370	$-287.201^{+00.738}_{-00.743}$	$-431.642^{+00.125}_{-00.126}$	$162.828^{+00.208}_{-00.209}$
NGC 4590	−2.23	299.626	36.051	0.066 ± 0.003	−2.764 ± 0.005	1.792 ± 0.004	−95.200 ± 0.400	$241.037^{+07.875}_{-08.491}$	$38.792^{+01.815}_{-01.957}$	$44.535^{+03.181}_{-03.430}$
NGC 4833	−1.85	303.604	−8.015	0.116 ± 0.001	−8.315 ± 0.004	−0.937 ± 0.003	207.860 ± 0.570	$162.823^{+02.565}_{-02.609}$	$-343.040^{+01.647}_{-01.675}$	$-49.533^{+00.342}_{-00.348}$
NGC 5024	−2.10	332.963	79.764	0.014 ± 0.002	−0.147 ± 0.005	−1.351 ± 0.003	−64.330 ± NaN	$-210.222^{+23.143}_{-29.808}$	$-373.543^{+45.370}_{-58.437}$	$-123.105^{+07.449}_{-09.594}$
NGC 5897	−1.90	342.946	30.294	0.068 ± 0.003	−5.411 ± 0.005	−3.460 ± 0.005	99.920 ± 1.310	$59.398^{+05.665}_{-06.115}$	$-432.159^{+15.925}_{-17.191}$	$92.010^{+01.276}_{-01.377}$
NGC 5927	−0.49	326.604	4.860	0.100 ± 0.002	−5.047 ± 0.006	−3.233 ± 0.006	−115.700 ± 3.100	$245.275^{+03.456}_{-03.604}$	$-160.847^{+05.224}_{-05.449}$	$5.050^{+00.119}_{-00.124}$
NGC 6121	−1.16	350.973	15.972	0.500 ± 0.001	−12.496 ± 0.003	−18.979 ± 0.003	71.400 ± 0.300	$-51.995^{+00.042}_{-00.042}$	$-208.979^{+00.337}_{-00.338}$	$-6.028^{+00.041}_{-00.041}$
NGC 6144	−1.76	351.929	15.701	0.067 ± 0.004	−1.765 ± 0.009	−2.637 ± 0.006	195.850 ± 0.900	$-172.066^{+01.442}_{-01.626}$	$-235.134^{+13.225}_{-14.909}$	$29.886^{+01.532}_{-01.727}$
NGC 6171	−1.02	3.373	23.011	0.148 ± 0.003	−1.936 ± 0.006	−5.949 ± 0.005	−35.010 ± 0.890	$-13.350^{+00.627}_{-00.649}$	$-175.721^{+03.475}_{-03.600}$	$-68.295^{+00.992}_{-01.027}$
NGC 6287	−2.10	0.132	11.023	0.107 ± 0.005	−4.887 ± 0.012	−1.921 ± 0.008	−292.450 ± 0.810	$302.088^{+01.063}_{-01.164}$	$-182.244^{+09.082}_{-09.950}$	$73.588^{+05.558}_{-06.090}$
NGC 6333	−1.77	5.544	10.705	0.093 ± 0.003	−2.203 ± 0.008	−3.208 ± 0.006	229.100 ± 7.000	$-251.065^{+00.533}_{-00.565}$	$-161.491^{+5.960}_{-06.315}$	$52.160^{+00.241}_{-00.255}$
NGC 6356	−0.40	6.724	10.220	0.079 ± 0.007	−3.768 ± 0.010	−3.375 ± 0.006	27.000 ± 4.300	$-55.161^{+01.584}_{-01.873}$	$-275.756^{+23.089}_{-27.293}$	$89.281^{+06.258}_{-07.398}$
NGC 6362	−0.99	325.555	−17.570	0.097 ± 0.001	−5.501 ± 0.003	−4.742 ± 0.003	−13.000 ± 0.600	$157.839^{+01.845}_{-01.887}$	$-273.684^{+03.456}_{-03.535}$	$129.152^{+01.368}_{-01.400}$
NGC 6397	−2.02	338.165	−11.960	0.378 ± 0.001	3.291 ± 0.003	−17.591 ± 0.003	19.180 ± 0.460	$65.571^{+00.183}_{-00.183}$	$-140.694^{+00.313}_{-00.314}$	$-140.090^{+00.251}_{-00.252}$
NGC 6809	−1.94	8.793	−23.272	0.171 ± 0.001	−3.402 ± 0.003	−9.264 ± 0.003	176.460 ± 0.570	$-213.306^{+00.323}_{-00.327}$	$-232.168^{+01.827}_{-01.851}$	$-56.858^{+00.093}_{-00.094}$
NGC 6838	−0.78	56.746	−4.564	0.225 ± 0.001	−3.384 ± 0.003	−2.653 ± 0.003	−21.010 ± 0.530	$-69.004^{+00.385}_{-00.389}$	$-48.222^{+00.237}_{-00.239}$	$40.826^{+00.163}_{-00.165}$
NGC 7099	−2.27	27.179	−46.836	0.075 ± 0.004	−0.702 ± 0.006	−7.222 ± 0.006	−186.480 ± 0.930	$-50.296^{+08.275}_{-09.213}$	$-475.539^{+22.199}_{-24.714}$	$87.567^{+02.606}_{-02.901}$

This research has been supported by the Kennilworth Fund of the New York Community Trust. We also greatly appreciate the comments by Julie Lutz, Charli Sakari, Andrea Kunder, Dana Casetti-Dinescu, and Donald Serna-Grey on a preliminary draft of this manuscript.

References

Baade, W. 1944, ApJ, 100, 137
Baade, W. 1956, PASP, 68, 5
Bailer-Jones, C. A. L., Rybizki, J., Fouesneau, M., et al. 2018, AJ, 156, 58
Barbier-Brossat, M., Petit, M., & Figon, P. 1994, A&AS, 108, 603
Beers, T. C., Chiba, M., Yoshii, Y., et al. 2000, AJ, 119, 2866
Bersier, D., & Wood, P. R. 2002, AJ, 123, 840
Bhardwaj, A., Rejkuba, M., Minniti, D., et al. 2017, A&A, 605, A100
Chamberlain, J. W., & Aller, L. H. 1951, ApJ, 114, 52
Clement, C. M., Muzzin, A., Dufton, Q., et al. 2001, AJ, 122, 2587
Corwin, T. M., Sumerel, A. N., Pritzl, B. J., et al. 2006, AJ, 132, 1014
Deutsch, A. J. 1955, Principes Fondamentaux de la Classification Stellaire (Paris: CNRS)
Eggen, O. J., Lynden-Bell, D., & Sandage, A. R. 1962, ApJ, 136, 748
ESA 1997, The Hipparcos and Tycho catalogues. Astrometric and photometric star catalogues derived from the ESA Hipparcos Space Astrometry Mission Vol. 1200 (Noordwijk: ESA), 1
Gaia Collaboration 2018, A&A, 616, A12
Gonzalez, G., & Wallerstein, G. 1994, AJ, 108, 1325
Harris, H. C. 1981, AJ, 86, 719
Harris, H. C. 1985, AJ, 90, 756
Harris, W. E. 1996, AJ, 112, 1487
Helfer, H. L., Wallerstein, G., & Greenstein, J. L. 1959, ApJ, 129, 700
Johnson, D. R. H., & Soderblom, D. R. 1987, AJ, 93, 864
Kharchenko, N. V., Scholz, R.-D., Piskunov, A. E., et al. 2007, AN, 328, 889
Kinman, T. D. 1959, MNRAS, 119, 538
Koposov, S. 2016, Gal UVW
Kordopatis, G., Gilmore, G., Steinmetz, M., et al. 2013, AJ, 146, 134
Kovtyukh, V., Wallerstein, G., Yegorova, I., et al. 2018a, PASP, 130, 054201
Kovtyukh, V., Yegorova, I., Andrievsky, S., et al. 2018b, MNRAS, 477, 2276
Lemasle, B., Kovtyukh, V., Bono, G., et al. 2015, A&A, 579, A47
Luri, X., Brown, A. G. A., Sarro, L. M., et al. 2018, A&A, 616, A9
Lutz, T. E., & Kelker, D. H. 1973, PASP, 85, 573
Maas, T., Giridhar, S., & Lambert, D. L. 2007, ApJ, 666, 378
Martínez-Vázquez, C. E., Monelli, M., Bernard, E. J., et al. 2017, ApJ, 850, 137
McConnachie, A. W. 2012, AJ, 144, 4
Monelli, M., Fiorentino, G., Bernard, E. J., et al. 2017, ApJ, 842, 60
Myeong, G. C., Evans, N. W., Belokurov, V., Sanders, J. L., & Koposov, S. E. 2018, ApJL, 863, L28
O'Connell, D. J. K. 1958, American Journal of Physics, 27, 195
Samus, N. N., Kazarovets, E. V., & Durlevich, O. V. 2001, OAP, 14, 266
Schmidt, E. G., Johnston, D., Lee, K. M., et al. 2004, AJ, 128, 2988
Schmidt, E. G., Langan, S., Lee, K. M., et al. 2003a, AJ, 126, 2495
Schmidt, E. G., Lee, K. M., Johnston, D., et al. 2003b, AJ, 126, 906
Schwarzschild, M., Schwarzschild, B., Searle, L., et al. 1957, ApJ, 125, 123
Searle, L., & Zinn, R. 1978, ApJ, 225, 357
Soszyński, I., Udalski, A., Szymański, M. K., et al. 2008, AcA, 58, 293
Soszyński, I., Udalski, A., Szymański, M. K., et al. 2010, AcA, 60, 91
Willman, B. 2010, AdAst, 2010, 285454
Woolley, R. 1966, Obs, 86, 76